Journal of Global Environment Engineering, Vol. 15, pp.25-38, 2010

MODIFICATION OF FIRE MODULE IN LPJ-DGVM FOR APPLICATION IN TROPICAL AREA: A CASE STUDY OF WEST KALIMANTAN

Arno Adi KUNTORO[1*], Takao YAMASHITA[1] and Ade WAHYU[2]

[1]Graduate School for International Development & Cooperation, Hiroshima University.
(1-5-1 Kagamiyama, Higashi-Hiroshima 739-8529, Japan)
[2]Directorate General of Forestry Planning, Ministry of Forestry of Indonesia,.
(Manggala Wanabhakti Building, Block VII, 5th floor, Jl. Gatot Subroto - Jakarta 10270, Indonesia)
* E-mail: *arno-adikuntoro@hiroshima-u.ac.jp*

Within the last few decades, forest fire in Indonesia tends to intensify greatly with the largest event occurred in 1997-1998. Borneo (Kalimantan) is one of the islands in Indonesia which is largely affected by forest fire. In this study, a modified Lund Potsdam Jena Dynamic Global Vegetation Model (LPJ-DGVM) is used to simulate the effect of interannual climate variability and land cover type to forest fire occurrence especially in tropical area. Two interannual climate variability indices are included into the model: MEI and DMI which represents ENSO and IOD phenomena, respectively. In study case of West Kalimantan, simulation of hotspot intensity and distribution from 2002 to 2004 shows relatively good results compared to the data. Simulation of 3 schemes without considering interannual climate variability show *index of agreement* of 0.389, 0.602 and 0.744, while simulation of 3 schemes with considering interannual climate variability show *index of agreement* of 0.761, 0.755 and 0.761. This study suggests that forest fire prediction using process-based model which includes the factors of climatology, land cover and interannual climate variability might be useful for regional future forest management to minimize forest loss due to forest fire, especially in tropical area such as Borneo Island.

Key Words: *DGVM, forest fire, land cover, interannual climate variability, Kalimantan*

1. INTRODUCTION

Land cover change which is mainly associated with forest loss contributes to about 25% of the total anthropogenic CO_2 to the atmosphere[1]. In this case, Indonesia is one of the countries with the largest forest area, but ironically, is also one of the countries with the largest forest loss in the world[2]. Analysis from satellite data within the last few years shows that forest fire in Borneo Island tends to increase especially in degraded forests[3),4)]. Forest degradation in Indonesia is mostly caused by uncontrolled logging activities, access road building, forest conversion to farmland or industrial plantation and also the use of fire for land clearing. Those activities might increase fire prone area in formerly forest ecosystem and lead to a higher forest fire intensity especially in extreme interannual climate variability events, such as El-Niño[5),6)]. Many studies show that forest fire in Borneo Island has strong correlation with El Niño event[7),8),9)], although it does not always lead to higher number of hotspots/fire events[10)]. One of the largest forest losses in Indonesia occurred in 1997-1998 following an extreme El-Niño event, resulted in 8 million hectares of forest burning[5)], with 3 to 4.5 million hectares of forest loss in Borneo Island[8),10)]. Therefore, study on the terrestrial ecosystem together with climate characteristics might be useful to minimize forest loss due to forest fire in the future.

Forest fires can be divided into three types: underground fires, surface fires and crown fires. While underground fire generally occurs in wetland/peatland, dryland tropical forests damaged

mostly by surface fire[7]. In Kalimantan Island, both type of forests are exist, and both are damaged by fires. For regional scale analysis, simulation of fire occurrence needs to be conducted by considering the interaction between terrestrial ecosystem and the atmosphere.

Interaction between the terrestrial ecosystem and the atmosphere can be simulated by using a process based model such as Lund-Potsdam-Jena Dynamic Global Vegetation Model (LPJ-DGVM). LPJ-DGVM and its improved versions have been used to analyze global terrestrial carbon balance in the past/present conditions[11),12),13)] and for future predictions[14),15)]. This model has also been used to analyze other aspects than carbon balance, such as global runoff[16)] and global fire disturbance[17)].

The role of fire in the global carbon cycle has been widely recognized since the last few decades so it is common that fire module is included in many earth system models[18)]. In the early version of LPJ-DGVM (LPJ v1), fire disturbance is computed as function of litter carbon availability, upper soil moisture, length of fire season and other specific Plant Functional Type (PFT) parameters[17),12)]. The module was developed based on forest fire events in Portugal, Australia and United States, which might have different characteristics with forest fire in tropical area such as Borneo Island. For example, it is common in Borneo Island that fire event (hotspot) occurred simultaneously in large area with low tendency to spread to another point[6),7)], while in another place fire might tend to spread from one point to another as influenced by climatology condition, topography, litter characteristics, etc.[19),20)].

Most studies using LPJ-DGVM are conducted in 0.5° x 0.5° grid with monthly climatology data input. In LPJ v1, linear interpolation is used to provide daily data from monthly data. Monthly precipitation data is distributed into daily precipitation using an empirical equation as function of number of rain days in each month. However, model application in daily time step using daily data significantly increases the computation time and data size. Two alternative ways can be used: by using advance computing system for large scale analysis or by using common system for smaller scale analysis. For the first case, an application for parallel computer system which provides daily time step computation using daily climatology data for global scale analysis has been developed by Venevsky and Maksyutov[21)]. For the second case, specific area analysis can be used as study case.

Finally, modification of LPJ-DGVM in vegetation growth characteristics, such as establishment stages, average tree size (height and diameter), photosynthesis rate and fire are important to analyze the interaction between atmosphere-biosphere in regional scale especially in tropical area such as Borneo Island.

2. MATERIAL AND METHODS

(1) Overview of LPJ-DGVM

Continuous improvements from the early version of LPJ-DGVM (LPJ v1) have been conducted which resulted in several versions of LPJ-DGVM such as LPJmL and LPJml v3. LPJmL is an improved version that focuses on agricultural plants and crops functional types, while LPJmL v3 focuses on river routing and irrigated agriculture. In this study, a modification of LPJ v1 is used to analyze forest fire occurrence in tropical area.

LPJ-DGVM is a 1-dimensional model, i.e., no interaction is considered among neighboring grids. Each grid represents an area which might be occupied by several PFTs. LPJ v1 uses monthly climatology data which consists of mean temperature, precipitation, number of rain-days in a month, cloud cover, annual global atmospheric CO_2 concentration and global soil type. **Figure 1** shows the flowchart of LPJ v1 and the modified LPJ v1 used in this study. In this study, 0.25°x 0.25° degree grid is used instead of 0.5° x 0.5° degree grid and daily climatology data is used instead of monthly data. Daily data for this study is derived from NCEP/NCAR Reanalysis Project (NNRP) data (http://www.cdc.noaa.gov/data/gridded/data.ncep.reanalysis.html) together with precipitation data from Tropical Rainfall Measuring Mission (TRMM) (http://disc2.nascom.nasa.gov/Giovanni/tovas/TRMM_V6.3B42_daily.2.shtml)

Daily *Potential Evapo-Transpiration (PET)* and daily *Photosynthetic Active Radiation (PAR)* in LPJ-DGVM are computed using temperature data, latitude, daylight hours and approximation of net radiation. *Gross photosynthesis* is computed from two potential sources: the light limited photosynthesis and the *rubisco* limited photosynthesis. *Autotrophic respiration* demand consists of two parts: maintenance and growth respiration. *Maintenance respiration* is computed as function of temperature and total amount of biomass in vegetation parts (leaf, wood and root). *Growth respiration* is computed as constant fraction of gross photosynthesis. *Net photosynthesis* is computed as the difference between gross photosynthesis and total autotrophic respiration. LPJ-DGVM uses three main carbon pools: vegetation, litter and soil pools. During the life of the vegetation, some fraction of carbon is transferred from one pool to another. For example,

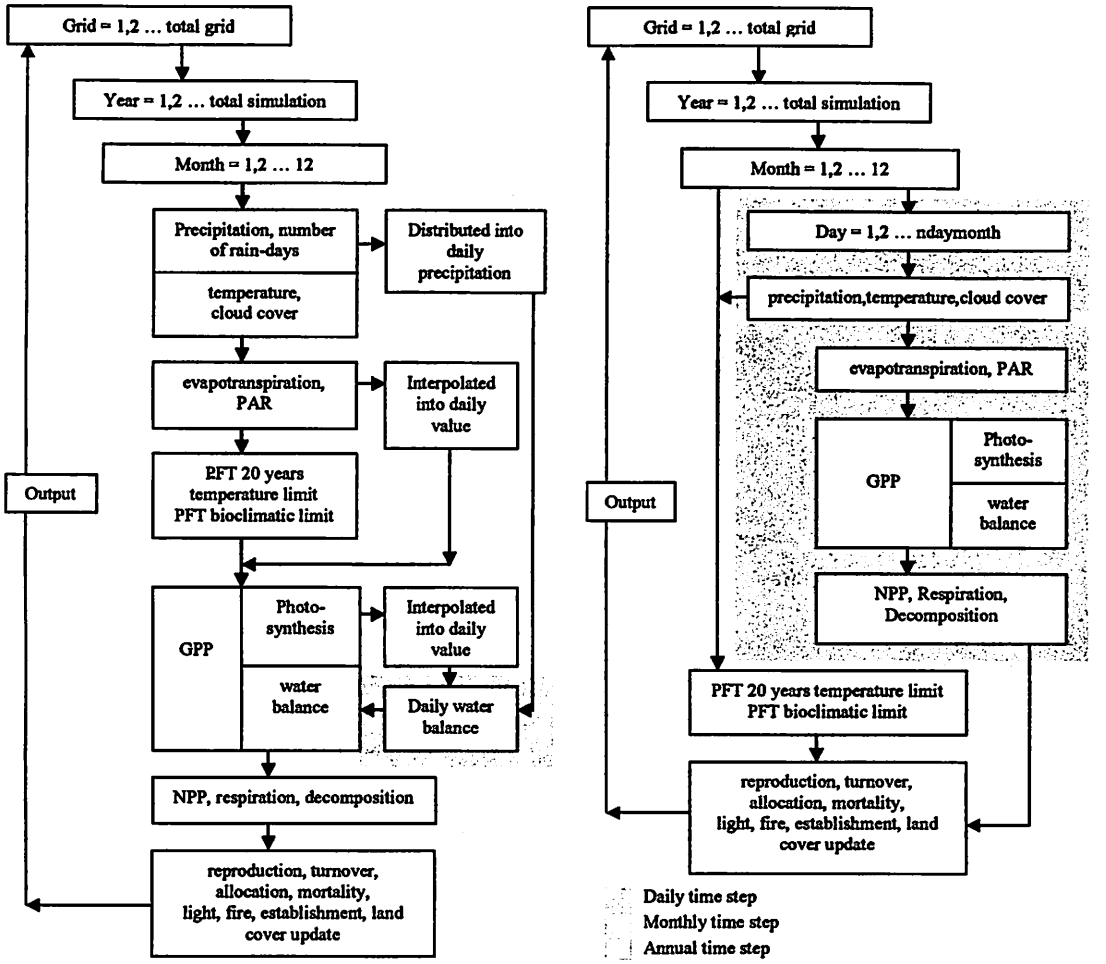

a) Flowchart of LPJ-v1

b) Flowchart of Modified LPJ-v1 for this study

Figure 1 Flowchart of LPJ-DGVM

carbon from leaf and root is transferred into litter, from sapwood into heartwood, from litter into soil, from soil into atmosphere, etc. *Reproduction* which counts the amount carbon used to produce plant's reproductive organs is taken as a constant fraction of net photosynthesis. After all demands are fulfilled, the remaining carbon is used for vegetation growth.

Vegetation reduction can be resulted from *light* competition, low growth efficiency, high temperature and *natural fire*. To represent the *anthropogenic land cover change, vegetation coverage* in each grid is updated using land cover map. Anthropogenic land cover change is assumed to occur if land cover data in an area shows the reduction of woody vegetation after all natural changes are computed in the previous section. In this case, wood carbon is assumed to be harvested and taken away from the ecosystem.

(2) Study Area

West Kalimantan is one the provinces of Indonesia in Borneo Island which is crossed by the equator. This province lies between 2°08'N to 3°05'S and 108°00'E to 114°10'E, covers an area of 146,807km^2 which occupies about 20% of the total area of the island. Most area of West Kalimantan is lowland with some main rivers and hundreds of small rivers. Main rivers in this area such as Kapuas and Melawi River are commonly used for transportation. Kapuas River is considered as the longest river in Indonesia with length of more than 1,000km. Mountainous area lies in the east and south east border of this province with the highest peak of more than 2,200m from mean sea level. **Figure 2** shows topographical feature of Borneo Island and West Kalimantan. The climate in this area is characterized by high precipitation rate and high temperature throughout the year. West Kalimantan has monsoon

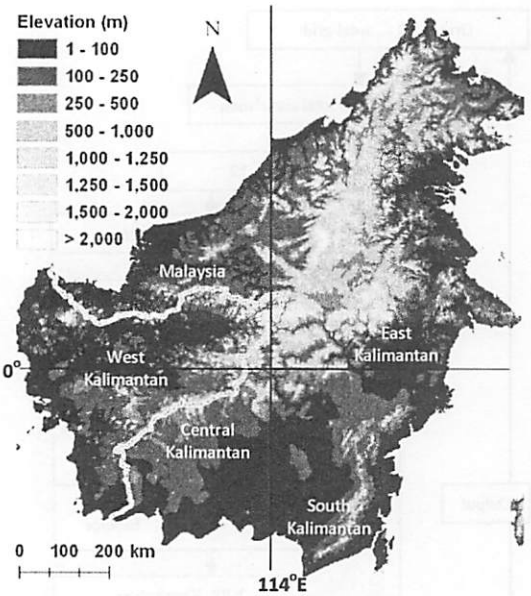

Figure 2 Topograpy map* of Borneo Island and West Kalimantan
* *source: http://hydrosheds.cr.usgs.gov/*

type climate with two seasons: dry season from April to September and rainy season from October to March. Dry season is influenced by the south monsoon from the Australian Continent, while rainy season is influenced by the north monsoon from the Asia Continent and the north Pacific.The mountainous area in the east part receives more precipitation compared to the lowland area in the west and south part. Data from three meteorological stations: Supadio (Pontianak), Sintang and Putussibau from 1996 to 2007 shows that the annual precipitation were ranges from about 3,100mm (Supadio and Sintang) to about 3,800mm (Putussibau). The minimum and maximum average monthly precipitation from the three stations were 151 mm (August) and 416 mm (January), respectively. Average annual air temperature were 23.0°C for daily minima and 32.4°C for daily maxima. The average minimum and maximum monthly temperature from the tree stations were 22.5°C (July) and 33.1°C (May/June), respectively.

Land cover data from Ministry of Forestry Republic of Indonesia is used in this study. The data is derived from *LandSat* image, validated with ground check and updated once in four years. **Figure 3a** shows land cover map of West Kalimantan in 2004. The most dominant land cover in this area was dry farmland, located in the west to centre part. Most dryland forests was located in the east and south east, while most wetland/wetland forests was located near coastal area in the west part and in the area of Sentarum Lake National Park in the north east. Wetlands is closely related to peatlands since about 75% of wetlands area can be categorized as peatlands[22]. **Figure 3b** shows the averaged land cover map with following criteria: >75% primary forest, >50% secondary/primary forest, >50% dry farmland, >75% dry farmland, >50% bush, grass and bareland and >50% wetland/peatland. The averaged map is used in further computation since LPJ-DGVM consider PFT distribution in each grid as "fractional coverage", that is, one grid might consist of different PFT and coverage area, without considering the exact location of each PFT within the grid. **Figure 3c** shows hotspot data in West Kalimantan during El-Niño period from 2002 to 2004. Most hotspots appeared in the centre and the south part of this area. **Figure 3d** shows average monthly number of hotspot together with average monthly precipitation. In general, forest fire occurred during dry season and the data shows that most hotspots were detected in August and September. **Figure 3e** shows total area per land cover type in 2004. The data shows that almost 48% of the total area in West Kalimantan was farmland (around 7.0 milion ha). Dryland forests (both primary and secondary) covered almost 28% of the total area (around 4.0 milion ha), while wetland/peatland/swamp and wetland/peatland forest (both primary and secondary) covered almost 11% of the total area (around 1.6 million ha). Other land cover type such as grassland, bush and bareland covered almost 13% of the total area (around 1.9 milion ha). Nowadays, satellite-derived hotspot data from AVHRR NOAA, SPOT and MODIS is widely used for forest fire analysis. For this study, hotspot data from Ministry of Forestry which is compiled from AVHRR NOAA is used. The data comprises both location and time of occurrence of each hotspot in daily based. **Figure 3f** shows average annual number of hotspot in West Kalimantan from 2002-2004. Within this period, the data shows that most hotspot appeared in dry farmland, with more than 6,000 hotspots occurrence in a year. However, further analysis shows that dry farmland might be not the most fire-prone land cover type in West Kalimantan. **Figure 3g** shows that wetland/peatland/swamp, bareland and bush had more hotspots per square area compared to the other land cover types. For example, in average of 1000 hectare of wetland/peatland/swamp, about 2.09 hotspots were detected per year, while only 0.94 hotspots were detected in dry farmland. Based on this preliminary analysis, further modification of LPJ-DGVM is focused on computation of the tendency of fire occurrence and total burned area, by considering land cover type (forests, farmland, wetland/peatland/swamp and bush/bareland), soil water and interannual climate variability.

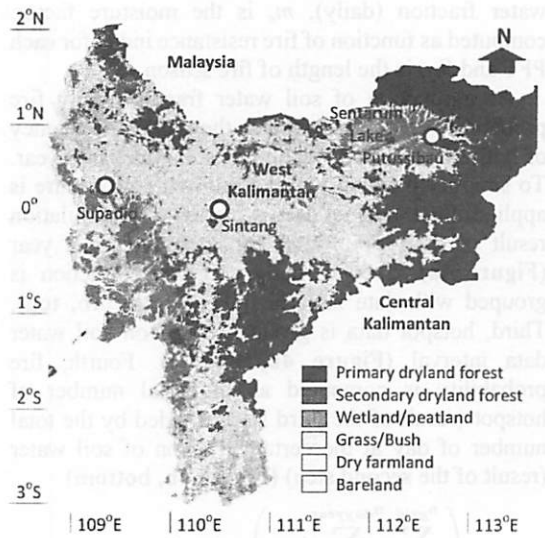

a.Land cover map (2004)

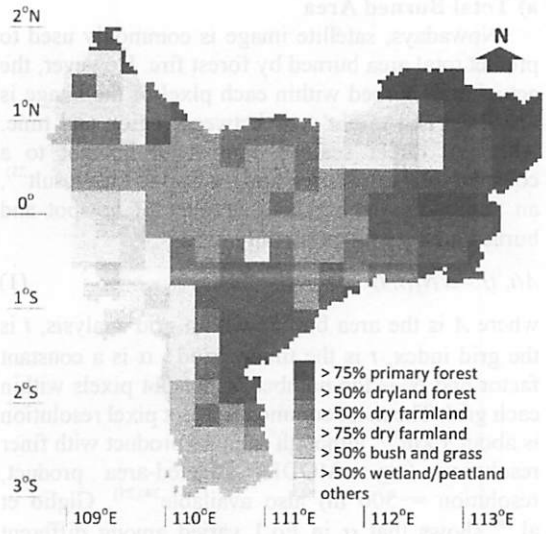

b. averaged land cover in 0.25° square grid

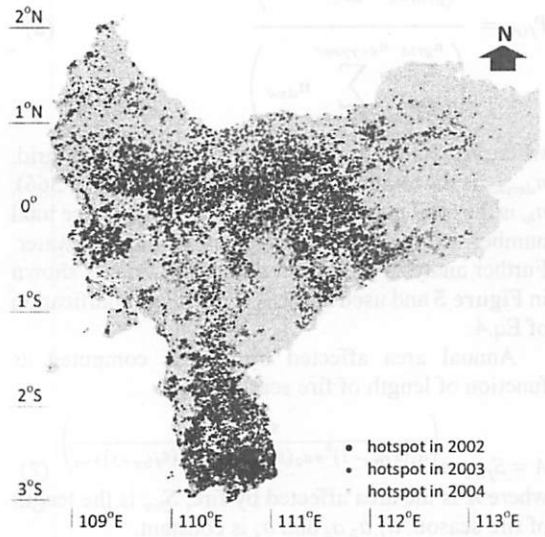

c. Hotspot in 2002 to 2004

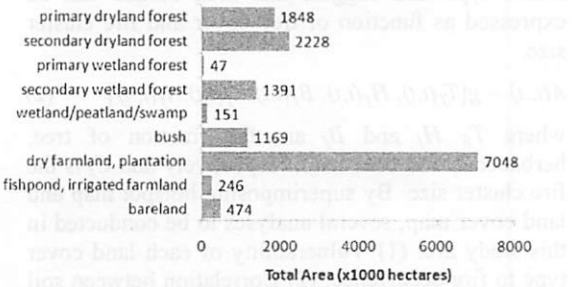

e. Land cover area (2004)

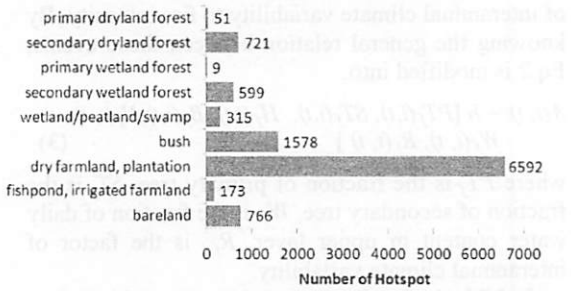

f. Average number of hotspot per year (2002-2004)

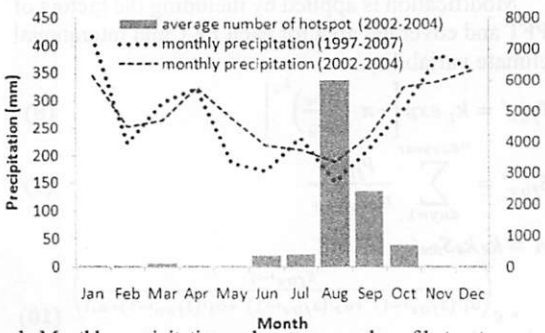

d. Monthly precipitation and average number of hotspot

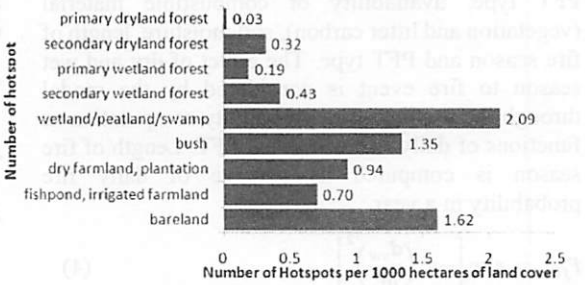

g. Average number of hotspot per land cover area (2002-2004)

Figure 3 Land cover, hotspot and precipitation data of West Kalimantan

(3) Model Modification

a) Total Burned Area

Nowadays, satellite image is commonly used to predict total area burned by forest fire. However, the actual area burned within each pixel of the image is unknown and might vary between region and time. Although direct scaling number of hotspot to a constant total area burned might lead to bias result[23], an approach which relates number of hotspot and burned area is still commonly used.

$$A(i, t) = \alpha N_f(i, t) \quad (1)$$

where A is the area burned within grid analysis, i is the grid index, t is the time period, α is a constant factor and N_f is the number of hotspot pixels within each grid. The most common hotspot pixel resolution is about 1 km[10], although satellite product with finer resolution (e.g.: MODIS affected-area product, resolution = 500 m) also available[24),25]. Giglio et al.[18] shows that α in Eq.1 varied among different biome type and suggest that area burned can be expressed as function of tree cover and fire cluster size.

$$A(i, t) = g[T_f(i,t), H_f(i,t), B_f(i,t), C_f(i,t), N_f(i, t)] \quad (2)$$

where T_f, H_f and B_f are the fraction of tree, herbaceous and bare land, respectively and C_f is the fire cluster size. By superimposing hotspot map and land cover map, several analyses to be conducted in this study are: (1) Vulnerability of each land cover type to fire occurrence, (2) Correlation between soil water content and fire occurrence and (3) The effect of interannual climate variability to fire intensity. By knowing the general relation between those events, Eq.2 is modified into:

$$A(i, t) = h\,[PT_f(i,t), ST_f(i,t), H_f(i,t), B_f(i,t), N_f(i, t), W_f(i, t), R_f(i, t)] \quad (3)$$

where PT_f is the fraction of primary tree, ST_f is the fraction of secondary tree, W_f is the fraction of daily water content in upper layer, R_f is the factor of interannual climate variability.

In LPJ v1, fire disturbance is computed based on PFT type, availability of combustible material (vegetation and litter carbon), soil moisture, length of fire season and PFT type. The effect of dry and wet season to fire event is considered by the model through the use daily fire probability computation as functions of daily soil water and PFT. Length of fire season is computed as average of daily fire probability in a year.

$$P_{fire} = exp\left[-\pi \left(\frac{d_{sw}}{m_e}\right)^2\right] \quad (4)$$

$$S_{fire} = \sum_{d=1}^{n_{dayyear}} \frac{P_{fire}}{n_{dayyear}} \quad (5)$$

where P_{fire} is the daily fire probability, d_{sw} is the soil water fraction (daily), m_e is the moisture factor, computed as function of fire resistance index for each PFT and S_{fire} is the length of fire season.

As a function of soil water fraction, daily fire probability can be assumed as the relative frequency of hotspot at certain fraction of soil water in a year. To simplify the analysis, the following procedure is applied. First, hotspot data is plotted with simulation result of daily soil water for each grid in a year (**Figure 4a**). Second, daily soil water fraction is grouped with data interval 0.05. (**Figure 4b, top**). Third, hotspot data is grouped based on soil water data interval (**Figure 4b, middle**). Fourth, fire probability is computed as the total number of hotspot (result of the third step) divided by the total number of day at the certain fraction of soil water (result of the second step) (**Figure 4b, bottom**).

$$P_{fire} = \frac{\left(\sum_{grid=1}^{n_{grid}} \sum_{d=1}^{n_{dayyear}} n_{hs}\right)}{\left(\sum_{grid=1}^{n_{grid}} \sum_{d=1}^{n_{dayyear}} n_{dsw}\right)} \quad (6)$$

where n_{grid} is the total number of computation grid, $n_{dayyear}$ is the total number days in a year (365 or 366), n_{hs} is the total number of hotspots and n_{dsw} is the total number of day at certain fraction of soil water. Further analysis of hotspot data using Eq.6 is shown in **Figure 5** and used as basis for further modification of Eq.4.

Annual area affected by fire is computed as function of length of fire season:

$$A = S_{fire} \cdot e^{\left(\frac{S_{fire}-1}{a_1(S_{fire}-1)^3+a_2(S_{fire}-1)^2+a_3(S_{fire}-1)+a_4}\right)} \quad (7)$$

where A is the area affected by fire, S_{fire} is the length of fire season, a_1, a_2, a_3 and a_4 is constant.

b) PFT and coverage area

Modification is applied by including the factors of PFT and coverage area for each PFT and interannual climate variability.

$$P_{fire}' = k_1\, exp\left[-\pi \left(\frac{d_{sw}}{m_e}\right)^{k_2}\right] \quad (8)$$

$$S_{fire}' = \sum_{day=1}^{n_{dayyear}} \frac{P_{fire}'}{n_{dayyear}} \quad (9)$$

$$A' = k_3 k_4 S_{fire}' * e^{\left(\frac{S_{fire}'-1}{a_1'(S_{fire}'-1)^3+a_2'(S_{fire}'-1)^2+a_3'(S_{fire}'-1)+a_4'}\right)} \quad (10)$$

where P_{fire}' is the modified fire probability, k_1 and k_2 are the function of PFT and coverage area, k_3 is the correction factor due to interannual climate

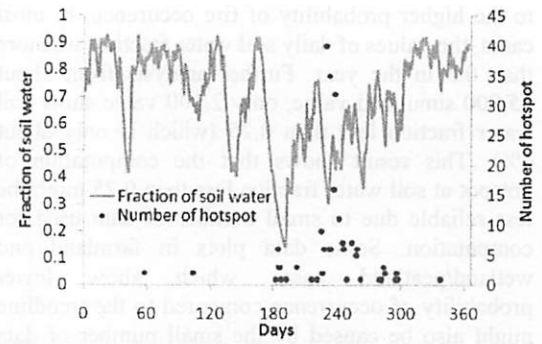

a. average fraction of soil water and number of hotspots

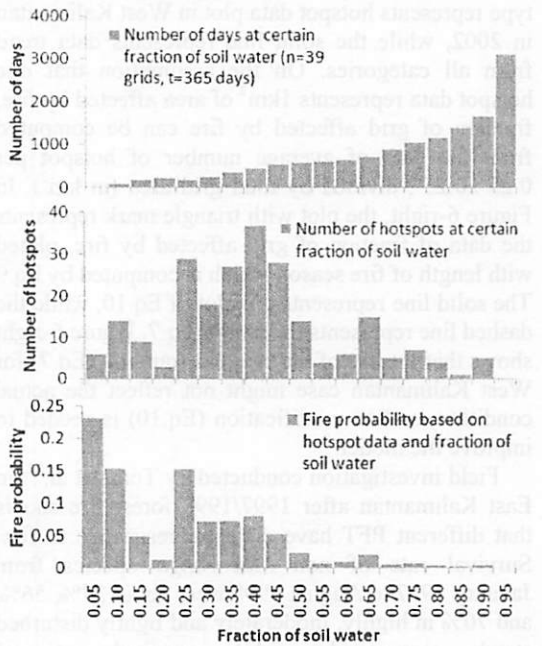

b. computation of fire probability based on hotspot data and fraction of soil water

Figure 4 Example of fire probability computation (using grid data with 50% area covered with dryland forest, n=39 grids, t=365 days in 2002)

variability, k_4 is the correction factor for length of fire season, A' is the modified affected area, a_1', a_2', a_3' and a_4' is constant.

c) Interannual climate variability

Two interannual climate variability phenomena are included into the modified model: The El Niño–Southern Oscillation (ENSO) and The Indian Ocean Dipole (IOD). The El Niño–Southern Oscillation (ENSO) is a fluctuation of the ocean-atmosphere conditions in the tropical Pacific which is mainly characterized by anomaly of sea surface temperature (SST), sea level pressure (SLP), surface wind and outgoing longwave radiation (OLR). One of the indices which describe the phase and intensity of ENSO phenomena is Multivariate ENSO Index (MEI). MEI is an index derived from six observed variables from Comprehensive Ocean-Atmosphere Data Set (COADS) over the tropical Pacific. Those variables are: sea level pressure, zonal and meridional wind component, sea surface temperature, surface air temperature and total cloudiness[26),27),28)].

Indian Ocean Dipole (IOD) is a fluctuation of the ocean-atmosphere conditions in the Indian Ocean which is mainly characterized by anomaly of SST and surface wind. IOD is associated by two patterns. First pattern is characterized by negative SST anomaly in the eastern Indian Ocean (western Sumatera Island) and positive SST in the western Indian Ocean (eastern Africa). First pattern is followed by low rainfall in Indonesian Archipelago and high rainfall in eastern Africa. Second pattern is characterized by the opposite conditions: high rainfall over Asian monsoon and low rainfall in eastern Africa. An index describing SST anomaly differs between (50°E – 70° E, 10°S – 10°N) and (90°E – 110°E, 10°S – 0°S) being referred as Dipole Mode Index (DMI), is used to indicate phase and intensity of this phenomena[29),30)].

Comparison between the total area burn and the interannual climate variability indices (MEI and DMI) shows that larger area is burnt during the warm period than during the cold period. To include interannual climate variability effect into the model, a simple power function $y = a\,x^b$, is applied as k_3 in Eq.(10).

$$k_{enso} = k_5^{MEI} \tag{11}$$

$$k_{iod} = k_6^{DMI} \tag{12}$$

Combination between ENSO and IOD effect is simplified as:

$$k_{join} = 0.5\,(k_{enso} + k_{iod}) \tag{13}$$

where k_{enso} is the correction factor due to ENSO effect, k_{iod} is the correction factor due to IOD effect, k_5 and k_6 are constant.

d) Meteorological Data

In general, meteorological data from NNRP from 1948 to 2006 is used for the whole simulation, but for simulation from 1998 to 2006, NNRP precipitation data is replaced by TRMM data. Data interpolation into finer grids is conducted using procedure proposed by Zhao et al.[31)] which is used for interpolating coarse meteorological data of Data Assimilation Office (DAO) for computation of MODIS GPP and NPP in finer grids.

$$D_i = \cos^4\left(\left(\frac{\pi}{2}\right)\left(\frac{d_i}{d_{max}}\right)\right), i = 1,2,3,4 \tag{14}$$

$$W_i = D_i / \sum_{i=1}^{4} D_i \quad (15)$$

$$V = \sum_{i=1}^{4} W_i V_i \quad (16)$$

where D_i is the distance of the fine computation grid to the four surrounding NNRP grids, d_i is the great-circle distance between the computation grid and NNRP grids, d_{max} is the great-circle distance between NNRP grids, V_i is the variables value at the coarse grid and V is the interpolated value at the fine grid.

Preliminary analysis of NNRP precipitation data shows that the average monthly value is nearly the same with other data sources. However, in many cases, daily precipitation in NNRP data (d_{prec}) tends to be smaller but distributed in more rain days. To deal with this problem, additional procedure is applied. First, rainfall is assumed to be occurred only in a number of days equal to the average number of rain days in a month. Second, daily precipitation data in a month is sorted from maximum to minimum. Data with list number more than average of number of rain day is reduced into zero (dr_{prec}). Third, data with list number less than average number of rain days is normalized (d'_{prec}) using the following equations:

$$d'_{prec}(i) = \left(dr_{prec}(i) \sum_{i=1}^{nday} d_{prec}(i) \right) \Big/ \left(\sum_{i=1}^{nday} dr_{prec}(i) \right) \quad (17)$$

where $d'_{prec}(i)$ is the normalized daily precipitation, $dr_{prec}(i)$ is the "corrected" daily precipitation after the data with list number greater than number of rain day is reduced to zero, $d_{prec}(i)$ is the original NNRP daily precipitation data and *nday* is the number of days in a month.

3. APPLICATION OF MODIFIED LPJ-DGVM FOR STUDY CASE OF WEST KALIMANTAN

Figure 5 and **Figure 6** show hotspot data together with simulation result of soil water fraction and length of fire season. Figure 5 shows that different PFT with different coverage area might have different response to fire. For example, a small number of hotspots appear in primary forest, fair number in secondary forest and a large number in bush, grass and bareland. At the same level of soil water fraction, bush and grass PFT are more prone to fire than tree FPT. The dashed line shows the trend of relative frequency of hotspot as function of soil water fraction. In general, the lower soil water fraction lead to the higher probability of fire occurence. In most cases, the values of daily soil water fraction are more than 0.5 in the year. Further analysis from about 35,000 simulated value, only 2,100 value show soil water fraction less than 0.25 (which is only about 6%). This result shows that the computation of hotspot at soil water fraction less than 0.25 might be less reliable due to small number of data used for computation. Some data plots in farmland and wetland/peatland cases which show lower probability of occurrence compared to the trendline might also be caused by the small number of data used in this study. In Figure 6-left, the various dot type represents hotspot data plot in West Kalimantan in 2002, while the solid line represents data trend from all categories. On the assumption that one hotspot data represents 1km^2 of area affected by fire, fraction of grid affected by fire can be computed from the data of average number of hotspot per 0.25°x0.25°, divided by total grid area (in km^2). In Figure 6-right, the plot with triangle mark represents the data of fraction of grid affected by fire, ploted with length of fire season which is computed by Eq.9. The solid line represents the plot of Eq.10, while the dashed line represents the plot of Eq.7. Figure 6-right shows that the use of the original equation (Eq.7) for West Kalimantan case might not reflect the actual condition, so that modification (Eq.10) is needed to improve the model.

Field investigation conducted by Toma et al.[32] in East Kalimantan after 1997/1998 forest fire shows that different PFT have different resistance to fire. Survival rate of non *Macaranga* species from January 1997 to August 1998 were about 37%, 56%, and 70% in highly, moderately and lightly disturbed stands respectively, while survival rate of *Macaranga sp.*, which is a species of pioneer tree, were about 0%, 0%, and 8%, in highly, moderately and lightly disturbed stands respectively. Kiyono and Hastaniah[5] who observed 782 tree stands from 24 species of *Dipterocarp* tree in East Kalimantan described that average survival rate during 1997/1998 forest fire event is 43,2%. Based on this data, resistance index of primary tropical tree in LPJ-v1 is modified from 0.12 to 0.50, while pioneer tree is modified from 0.50 to 0.05. Further analysis on the data using Eq.8 results in the following equations:

$$k_1 = 0.10\,(df + bs)(1.0\,df + 1.8\,bs) \quad (18)$$

$$k_2 = 0.75\,(df + bs)(10.0\,df + 3.0\,bs) \quad (19)$$

where: df is the portion of dry farmland and bs is the portion of bush, bareland and wetland/peatland/swamp.

The model is calibrated using total area affected by fire in Borneo Island from 1998 to 2006, conducted by Langner and Siegert[10] while further

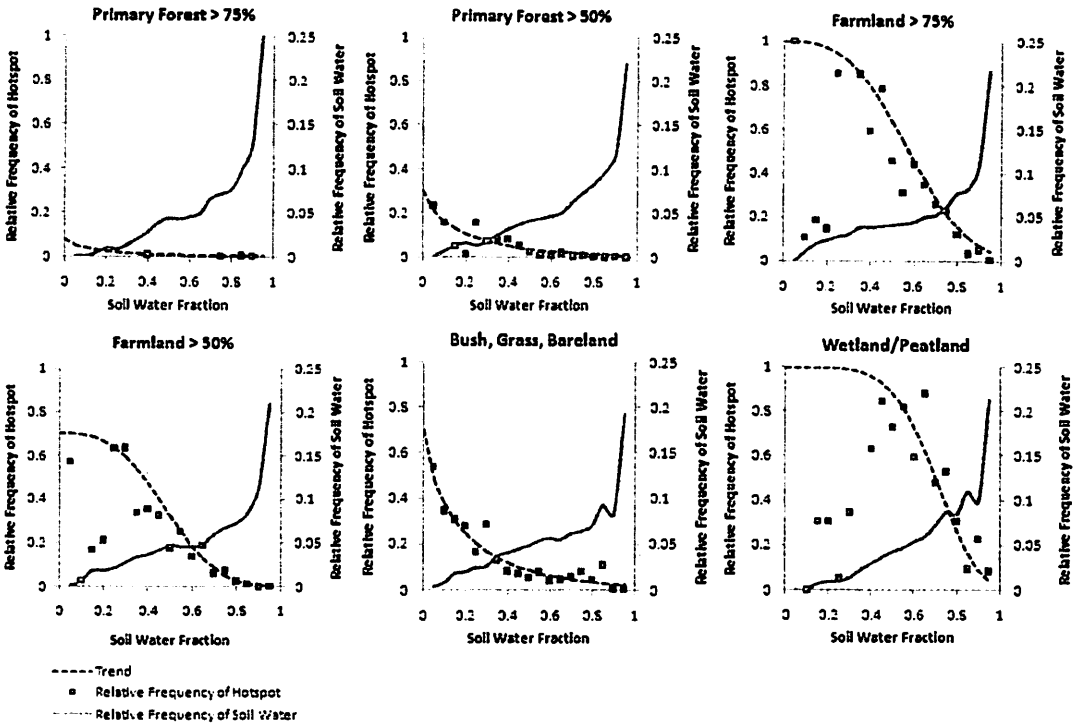

Figure 5 Fire and Soil Water Fraction Probability of Occurrence in West Kalimantan (2002) per 0.25° square grid

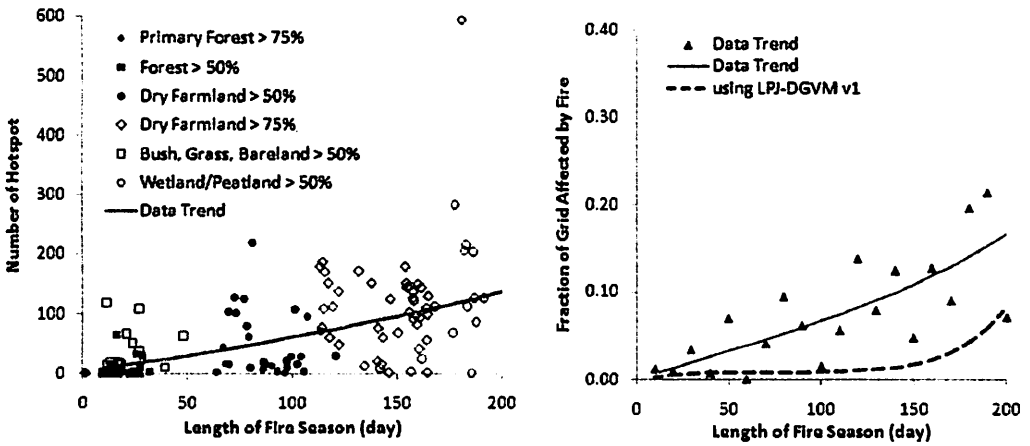

Figure 6 Number of hotspot and fraction area affected by fire

verification is conducted using hotspot data from Ministry of Forestry in West Kalimantan from 2002 to 2004. Figure 7 shows data of area affected by fire in Borneo Island.

Figure 8 shows MEI and DMI Index from 1997-2008. The positive value (light shaded) indicates the warm phase, while the negative value (dark shaded) indicates the cold phase. Comparison between interannual climate variability indices and area affected by fire shows that high intensity of forest fire usually appears during the warm phase of both ENSO and DMI. Optimization to find the appropriate function which represents the effect of ENSO and IOD to forest fire is conducted using index of agreement (*ioa)* as follow:

$$ioa = 1 - \frac{\sum_{j=1}^{J}\sum_{i=1}^{I}(S_j^i - O_j^i)^2}{\sum_{j=1}^{J}\sum_{i=1}^{I}(|S_j^i - M_o| + |O_j^i - M_o|)^2} \quad (20)$$

where S is the simulated value, O is the observed value, M_o is the average value of the data, I is the number of station/grid and J is the time.

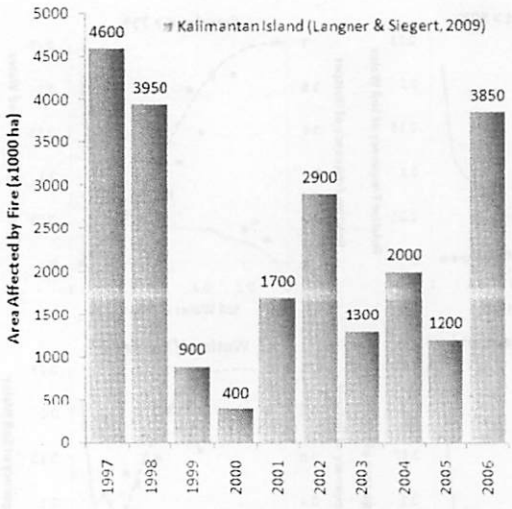

Figure 7 Area affected by fire in Borneo Island (1997-2006)

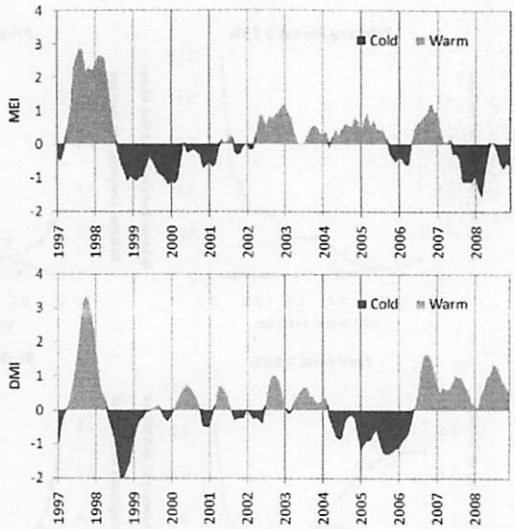

Figure 8 MEI and DMI index (1997-2009)

Table 1 Comparison of simulation result to the total area affected by fire in Borneo Island (1997-2006)

Years	Borneo Island Data*		Without considering ENSO/IOD						By considering ENSO/IOD					
			Scheme 1		Scheme 2		Scheme 3		Scheme 4		Scheme 5		Scheme 6	
	Area Burned (10^6ha)	% area burned	% area burned	|error|	% area burned	|error|	% area burned	|error|	% area burned	|error|	% area burned	|error|	% area burned	|error|
1997	4.6	6.27	0.94	0.063	2.60	0.037	5.29	0.010	10.08	0.038	13.05	0.068	11.56	0.053
1998	3.95	5.38	0.65	0.054	0.57	0.048	2.974	0.024	4.27	0.011	2.08	0.033	3.17	0.022
1999	0.9	1.23	0.71	0.012	0.75	0.005	3.954	0.027	2.70	0.015	3.43	0.022	3.07	0.018
2000	0.4	0.54	0.71	0.005	0.94	0.004	4.176	0.036	3.32	0.028	4.87	0.043	4.09	0.035
2001	1.7	2.32	0.77	0.023	1.42	0.009	5.263	0.029	4.85	0.025	5.53	0.032	5.19	0.029
2002	2.9	3.95	0.80	0.040	2.65	0.013	6.034	0.021	7.76	0.038	7.23	0.033	7.50	0.035
2003	1.3	1.77	0.78	0.018	2.14	0.004	5.428	0.037	6.62	0.048	6.76	0.050	6.69	0.049
2004	2	2.72	0.78	0.027	1.93	0.008	5.438	0.027	6.54	0.038	4.33	0.016	5.44	0.027
2005	1.2	1.63	0.76	0.016	1.23	0.004	4.732	0.031	5.37	0.037	2.32	0.007	3.85	0.022
2006	3.85	5.25	0.87	0.052	3.28	0.020	6.797	0.016	7.79	0.025	8.48	0.032	8.13	0.029
	average	**3.11**	**0.78**	**0.031**	**1.75**	**0.015**	**5.01**	**0.026**	**5.93**	**0.030**	**5.81**	**0.034**	**5.87**	**0.032**
	r			**0.534**		**0.519**		**0.234**		**0.696**		**0.560**		**0.642**

**Langner and Siegert[14]*

Table 2 Comparison of simulation result to hotspot intensity and distribution data in West Kalimantan (2002-2004)

Years	*Index of agreement (ioa)*					
	Without considering ENSO/IOD			By considering ENSO/IOD		
	Scheme 1	Scheme 2	Scheme 3	Scheme 4	Scheme 5	Scheme 6
2002	0.401	0.578	0.742	0.761	0.760	0.761
2003	0.383	0.706	0.819	0.833	0.833	0.833
2004	0.376	0.519	0.661	0.675	0.619	0.661
2002-2004	0.389	0.602	0.744	0.761	0.755	0.761

The *Microsoft Excel Solver Tool* uses the Generalized Reduced Gradient (GRG2) nonlinear optimization code developed by Leon Lasdon, University of Texas at Austin, and Allan Waren, Cleveland State University. This tool is used to find the optimum values for k_4, k_5 and k_6 in Eq.10 to Eq.12 and a_1',a_2',a_3' and a_4' in Eq. 10. Optimization is conducted by comparing the results with total area burnt in Borneo Island from Langner and Siegert[10]. Total area burnt in West Kalimantan is assumed as total area of West Kalimantan divided by total area of Borneo Island, mulitiplied by total area burnt for the

whole island.

The optimization is conducted using two criterias: maximum value of correlation coefficient and minimum value of error. The optimum value for k_4, k_5 and k_6 resulted from this procedure are 0.5, 1.542 and 2.0, respectively. In LPJ v1, a_1,a_2,a_3 and a_4 in Eq.7 is 0.45, 2.83, 2.96, and 1.04 respectively, while the optimum value for a_1',a_2',a_3' and a_4' in Equation 10 is 0.45, 2.83, 2.50, and 1.50 respectively.

Table 1 shows simulation results of total area burned from 1998-2006 with different scheme of modifications. **Scheme 1** is the simulation using original LPJ v1 equations without modification. **Scheme 2** is the simulation with modification only on fire probability index (Eq.9), while **scheme 3** is the simulation of scheme 2 with additional modification of area affected by fire (Eq.10). **Scheme 4, 5 and 6** are the simulations of scheme 3 with additional correction factor of ENSO, IOD and ENSO-IOD, respectively. In general, simulation results by considering ENSO/IOD show relatively higher correlation coefficient (0.696, 0.560 and 0.642) compared to simulation results without considering ENSO/IOD (0.534, 0.519 and 0.234). However, simulation results without considering ENSO/IOD show relatively lower average error (0.031, 0.015 and 0.026) compared to simulation results with considering ENSO/IOD (0.030, 0.034 and 0.032). From these results, it seems that the suitable modification scheme still cannot be concluded by only considering total area burned so that further analysis is conducted by simulating the spatial distribution of the fires in West Kalimantan during 2002-2004.

Table 2 shows simulation result of fire/hotspot distribution in West Kalimantan. Simulation results from 2002 to 2004 without considering ENSO/IOD show relatively lower index of agreement (0.389, 0.602 and 0.744) compared to the simulation by considering ENSO/IOD (0.761, 0.755 and 0.761).

Simulation results can be seen clearly in **Figure 9**. Hotspot data from 2002-2004 (Figure 3c) which is grouped into 0.25°x0.25° grid (Figure 9a) is used for comparison. Simulation of scheme 1 shows very low fire intensity in all type of land cover (Figure 9b). Although scheme 2 result shows relatively low error (see Table 1), this scheme tends to produce underestimate result in farmland area in the centre part of West Kalimantan (Figure 9c). Modification of area affected by fire is applied for scheme 3 to 6. This modification seems produce relatively similar spatial pattern with hotspot data. Although the result of scheme 3, 4 and 5 (figure 9d, 9e and 9f) show similar value, the use of correction factor of ENSO/DMI slightly enhance the results (see Table 2).

4. DISCUSSION AND CONCLUSION

Many dynamic vegetation models have been developed for various purposes and scales. LPJ-DGVM is one of the dynamic vegetation models which is originally developed for global scale analysis. In this study, a modified of LPJ-DGVM is used to simulate regional scale of wildfire intensity and distribution by considering climatology effect, land cover type and also interannual climate variability in tropical area. Photosynthesis, respiration, decomposition and water balance processes are computed using daily data in daily time step, while establishment, mortality, area affected by fire and other vegetation growth processes are computed in monthly or annual time step. Fire resistance characteristics of PFT are calibrated using data from large wildfire events which occurred in Borneo Island during 1997-1998. Computation of total area affected by fire is calibrated using satellite-derived data in Borneo Island from 1997 to 2006 while the simulation of fire intensity and distribution is verified using hotspot data in West Kalimantan from 2002 to 2004.

The modified fire module shows relatively good results in simulating fire intensity in various types of land cover and coverage areas. Forested areas are more resistance to fire, while bush, grassland and wetland/peatland are less resistance. Model result show that the area with high farmland coverage shows less resistance compared to the area with low farmland coverage, which is consistent with the fire occurrence data in Borneo Island especially in case of West Kalimantan.

Since the wildfires caused by anthropogenic activities such occurred in farmland are quite complex to be modeled, model results show relatively similar spatial pattern type despites the difference of climatology conditions and different years of simulation. Computation of total area affected by fire might also differ from the actual condition due to limitation in model spatial scale. The early version of LPJ-DGVM mainly developed for global-scale simulation, while this study is intended for regional or messoscale simulation. This study uses 0.25°x0.25° computation grid (about 27.5km x 27.5km) which is relatively coarse to include various effects of human disturbances such as the distance to road, village, etc. For example, in case study of Eastern Amazon, Cochrane[6] showed that forest area within 2km from deforested edge has fire rotation less than 20/year and highly increase after the distance of 2.5 km, with fire rotation more than 100/year. However, the distance of 2km is relatively small compared to

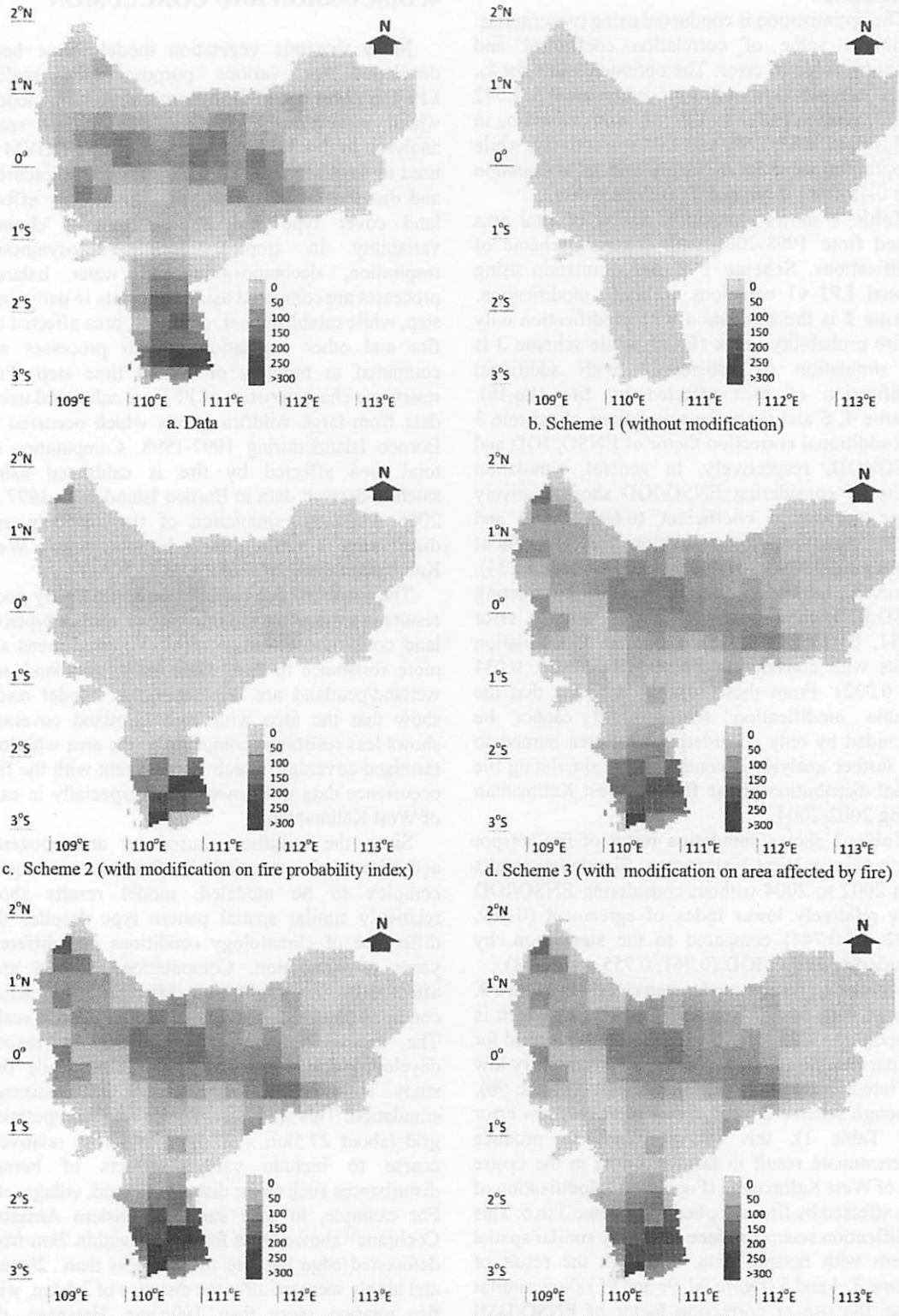

a. Data

b. Scheme 1 (without modification)

c. Scheme 2 (with modification on fire probability index)

d. Scheme 3 (with modification on area affected by fire)

e. Scheme 4 (with modification on fire probability index, area affected by fire and MEI)

f. Scheme 5 (with modification on fire probability index, area affected by fire and DMI)

Figure 9 Average number of hotspot in West Kalimantan and simulation result (2002-2004)

LPJ-DGVM grid size so that such effect could not be captured well in this model. LPJ-DGVM is a 1-D model. For better simulation of the impact of human activies, at least 2-D model in finer grid which considers the interaction of one grid to another surrounding grid should be used. However such computation is beyond the capability of this model.

Although in some period ENSO and IOD might have the same tendency, IOD is independent of ENSO[29]. During the cold period of IOD in 2004 to 2005, simulation result of scheme 5 (by considering IOD) shows less error compared to the result of scheme 4 (by considering ENSO). In the other simulation period from 1997 to 2003, simulation result of scheme 5 shows more error compared to the result of scheme 4. This comparison indicates that both ENSO and IOD might affect the fire occurrence in West Kalimantan and MEI/DMI can be used as one of the parameters in fire computation. However, the use of these indices might not be enough to describe the detail mechanism of fire occurrence in this area. Further study by considering the effect of each component which affect ENSO and IOD (e.g.: wind, SST, solar radiation) needs to be conducted for more detail analysis.

Many studies show that peat fire might release large amout of carbon to atmosphere[33),34)], however, prediction of carbon emission due to forest/pear fire is beyond the scope of this study. Further analysis of the effect of forest fire to the terrestrial carbon balance can be computed by relating total area affected by fire to the total carbon loss. However, this analysis should be conducted with cautions for each PFT and simulation years, especially in an area where interannual climate variability such as ENSO and IOD strongly affects the interaction pattern between the atmosphere and the terrestrial ecosystem. Finally, this study underlines the applicability of the modified LPJ-DGVM which includes climatology, interannual climate variability, land cover type and coverage area, for forest fire prediction in tropical area, such as West Kalimantan Province, Borneo Island.

REFERENCES

1) Denman, K.L., G. Brasseur, A. Chidthaisong, et al, P. Ciais, P.M. Cox, R.E. Dickinson, D. Hauglustaine, C. Heinze, E. Holland, D. Jacob, U. Lohmann, S Ramachandran, P.L. da Silva Dias, S.C. Wofsy and X. Zhang, 2007: *Couplings Between Changes in the Climate System and Biogeochemistry.* In: Climate Change 2007: The Physical Science Basis. Contribution of Working Group I to the Fourth Assessment Report of the Intergovernmental Panel on Climate Change [Solomon, S., D. Qin, M. Manning, Z. Chen, M. Marquis, K.B. Averyt, M.Tignor and H.L. Miller (eds.)]. Cambridge University Press, Cambridge, United Kingdom and New York, NY, USA.
2) FAO, *Global Forest Resources Assessment 2005: Progress towards sustainable forest management,* FAO, 2006.
3) Miettinen, J., Langner, A. and Siegert, F.: *Burnt area estimation for the year 2005 in Borneo using multi-resolution satellite imagery.* International Journal of Wildland Fire, Vol.16, 45-53, 2007.
4) Langner, A., Miettinen, J. and Siegert, F.: *Land cover change 2002–2005 in Borneo and the role of fire derived from MODIS imagery.* Global Change Biology, Vol.13, 2329-2340, 2007.
5) Kiyono, Y. and Hastaniah: *Phenological Observations at Bukit Soeharto Education Forest.* Ecological Studies: Rainforest Ecosystem of East Borneo, El Nino, Drought, Fire and Human Impact, Springer, 140, 121-128, 2000
6) Cochrane, M.A.: *Fire science for rainforests.* Nature, Vol.421, 913-919, 2003.
7) Mori, T.: *Effect of Drought and Forest Fires on Dipterocarp Forest in East Kalimantan.* Ecological Studies: Rainforest Ecosystem of East Borneo, El Nino, Drought, Fire, and Human Impact, Springer, 140, 29-45, 2000
8) Fuller, D.O., Jessup, T.C. and Salim, A.: *Loss of forest cover in Kalimantan, Indonesia, since the 1997-1998 El Niño.* Conservation Biology, Vol.18, No.1, 249-254, 2004.
9) Goldammer, J.G.: *History of equatorial vegetation fires and fire research inSoutheast Asia before the 1997–98 episode: A reconstruction of creeping environmental changes.* Mitig Adapt Strat Glob Change, Vol.12, 13-32, 2007.
10) Langner, A. and Siegert, F.: *Spatiotemporal fire occurrence in Borneo over a period of 10 years.* Global Change Biology, Vol.15, 48-62, 2009.
11) Lucht, W., Prentice, C., Myneni, R.B., et al.: *Climatic Control of the High-Latitude Vegetation Greening Trend and Pinatubo Effect.* Science, Vol.296, 1687-1689, 2002.
12) Sitch, S., Smith, B, Prentice, C. et al.: *Evaluation of ecosystem dynamics, plant geography and terrestrial carbon cycling in the LPJ dynamic global vegetation model.* Global Change Biology, 9, 161-185, 2003.
13) Bondeau, A., Smith, P.C., Zaehle, S. et al.: *Modelling the role of agriculture for the 20th century global terrestrial carbon balance.* Global Change Biology, 13, 679–706, 2007.
14) Lucht, W., Schaphoff, S., Erbrecht, T., et al.: *Terrestrial vegetation redistribution and carbon balance under climate change.* Carbon Balance and Management, I:6, 2006.
15) Morales, P., Hickler, T., Rowell, D.P., et al.: *Changes in European ecosystem productivity and carbon balance driven by regional climate model output.* Global Change Biology, Vol.13, 108-122, 2007.
16) Gerten, D., Schaphoff, S., Haberlandt U. et al. *:Terrestrial vegetation and water balance – hydrological evaluation of a dynamic global vegetation model.* Journal of Hydrology, 286, 249-270, 2003.
17) Thonicke, K., Venevsky, S., Sitch, S., et al.: *The role of fire disturbance for global vegetation dynamics: coupling fire into a Dynamic Global Vegetation Model.* Global Ecology & Biogeography, Vol.10, 661-677, 2001.
18) Giglio, L., van der Werf, G.R., Randerson, J.T., et al.: *Global estimation of burned area using MODIS active fire observations.* Atmospheric Chemistry and Physics, Vol.6, 957-974, 2006.
19) Sharples, J.J.: *Review of formal methodologies for wind–slope correction of wildfire rate of spread.* International Journal of Wildland Fire, Vol.17, 179-193, 2008.
20) Cruz, M.G. and Fernandes, P.M.: *Development of fuel models for fire behaviour predictionin maritime pine (Pinus pinaster Ait.) stands.* International Journal of Wildland Fire, Vol.17, 194-204, 2008.

21) Venevsky, S. and Maksyutov, S,: *SEVER: A modification of the LPJ global dynamic vegetation model for daily time step and parallel computation.* Environment Modeling & Software, Vol.22, 104-109, 2007.
22) Jauhiainen, J., Takahashi, H., Heikkinen, J.E.P., et al.: *Carbon fluxes from a tropical peat swamp forest floor.* Global Change Biology, 11, 1788-1797, 2005.
23) Kasischke, E.S., Hewson, J.H., Stocks, B., et al.: *The use of ATSR active fire counts for estimating relative patterns of biomass burning – a study from the boreal forest region.* Geophysical Research Letters, Vol.30 No.18, 10.1-10.4, 2003.
24) Roy, D.P., Jin, Y., Lewis, P.E., et al.: *Prototyping a global algorithm for systematic fire-affected area mapping using MODIS time series data.* Remote Sensing of Environment, Vol.97, 137-162, 2005.
25) Justice, C., Gigilio, L., Boschetti, L., et al.: *Algorithm Technical Background Document, MODIS Fire Product.* Version 2.3, 1 October 2006
26) Wolter, K. and Timlin, M.S.: *Measuring the strength of ENSO event: How does 1997/1998 rank?.*Weather, Vol.53 No.9, 315-324, 1998.
27) Wang, C., and Fiedler, P.C.: *ENSO variability and the eastern tropical Pacific: A review.* Progress in Oceanography, Vol.69, 239-266, 2006.
28) McPhaden, M.J., Zebiak, S.E. and Glantz, M.H.: *ENSO as an Integrating Concept in Earth Science.* Science, Vol.314, 1740-1743, 2006.
29) Saji, N.H., Goswami, B.N., Vinayachandran, P.N., et al: *A dipole mode in the tropical ocean Indian Ocean.* Nature, Vol.401, 360-363, 1999.
30) Saji, N.H., and Yamagata, T.: Possible impact of Indian Ocean Dipole mode events on global climate. Climate Research, Vol.25, 151-169, 2003.
31) Zhao, M., Heinsch, F.A., Nemani, R.R. et al.: *Improvement of the MODIS terrestrial gross and net primary production global data set.* Remote Sensing of Environment, 95, 164-176, 2004
32) Toma, T., Matius, P., Hastaniah et al.: *Dynamics of Burned Lowland Dipterocarp Forest Stands in Bukit Soeharto, East Kalimantan.* Ecological Studies: Rainforest Ecosystem of East Borneo, El Nino, Drought, Fire, and Human Impact, Springer, 140, 107-120, 2000.
33) Page, S.E., Siegert, F., Rieley, J.O., et al.: *The amount of carbon released from peat and forest fire in Indonesia during 1997,* Nature, Vol.420, 61-65, 2002.
34) Tacconi, L., Moore, P.F., Kaimowitz, D.: *Fires in tropical forests – what is realy the problem? Lesson from Indonesia.* Mitig Adapt Strat Glob Change, 12,55-66, 2007.

(Received January 19, 2010)